Politická ekonomie 2026

Volume 74 (1)
https://doi.org/10.18267/j.polek.1484
Open Access

PRAGUE UNIVERSITY OF ECONOMICS AND BUSINESS

Regional Disparities in Drivers and Peaking Pathways of CO_2 Emissions: Insights from Scenario Planning

Yang Yu, Yaping Gong, DooHwan Won, Atif Jahanger

Yang Yu (email: yuyang_0715@163.com; yuyang@hainanu.edu.cn), International Business School, Hainan University, Haikou, Hainan, China

Yaping Gong (email: *corresponding author*, gongyaping0830@126.com), International Business School, Hainan University, Haikou, Hainan, China

Doohwan Won (email: doohwan@pusan.ac.kr), Pusan National University, College of Economics and International Trade, Department of Economics, Pusan, Republic of Korea

Atif Jahanger (email: atif_jahanger@hotmail.com), International Business School, Hainan University, Haikou, Hainan, China

Abstract

Faced with domestic and international responsibilities, China urgently needs to coordinate various regions to achieve carbon peak in an orderly manner. As core regions driving economic expansion and primary hubs of energy consumption, the Beijing–Tianjin–Hebei (BTH) and the Yangtze River Delta (YRD) regions are substantial contributors to carbon emissions in China. To address regional disparities in carbon emission management, this study estimates CO_2 emissions from 1990 to 2021, employing the STIRPAT model to analyse influencing factors. The findings reveal that the key factor affecting CO_2 emissions in both regions is population. Energy intensity plays a larger role in the BTH, while urbanization affects the YRD more significantly and industrial structure notably affects emissions only in the YRD. Additionally, the PSO-SVR model is integrated with dynamic scenario analysis to predict carbon peaking under various scenarios. Predictions suggest peaks in 2026 for the BTH and 2028 for the YRD under a baseline scenario, with earlier peaks under low-carbon scenarios and delayed peaks under high-carbon scenarios. The research offers insights for region-specific carbon reduction management strategies, addressing regional disparities and guiding effective mitigation efforts.

Keywords: Carbon peaking, regional disparities, PSO-SVR model, dynamic scenario analysis, carbon reduction management strategies

JEL Classification: Q54, R11, C53, O13, Q43

Citation: Yu, Y., Gong, Y., Won, D., Jahanger, A.: Regional Disparities in Drivers and Peaking Pathways of CO2 Emissions: Insights from Scenario Planning. *Politická ekonomie,* 74(1), 170–197. https://doi.org/10.18267/j.polek.1484

1. Introduction

Climate change is a critical global issue (Yang *et al.*, 2023). As a key participant in advancing global ecological civilization, China has made addressing carbon emissions a national priority. China has pledged to realize the goals of "carbon peak and carbon neutrality", aiming to peak CO_2 emissions before 2030 and reach carbon neutrality by 2060 (Zhao *et al*., 2022; Y. M. Wei *et al.*, 2022). To meet the targets, China has undertaken practical measures (H. K. Wang *et al.*, 2019; Yu *et al.,* 2024). However, the accelerating pace of industrialization, urbanization and economic growth continues to drive a sustained increase in CO_2 emissions, which remains a significant challenge to achieving these goals.

Within the framework of China's regional economic development, the BTH and the YRD have garnered significant attention due to their strategic significance (M. Wei *et al*., 2024). The BTH comprises Beijing, Tianjin and Hebei provinces, forming an integrated cluster of provincial-level administrative regions with strong political, economic and cultural linkages. On the other hand, the YRD consists of Shanghai City as well as Anhui, Jiangsu and Zhejiang provinces, showing the characteristics of cross-regional coordinated development. Despite differences in their composition and governance models, these regions share notable similarities, offering a unique comparative foundation for examining their synergistic development and environmental impacts. The State Council's guidelines for achieving carbon peaking and carbon neutrality under the New Development Philosophy emphasized the coordinated advancement of the BTH and the integrated development of the YRD, alongside other key regional strategies. Moreover, the 14th Five-Year Plan highlighted that the pivotal regions for driving high-quality development are the BTH and the YRD. It can be seen that, as the hub of China's economic development and energy consumption, the Beijing–Tianjin–Hebei (BTH) and the Yangtze River Delta (YRD) regions play a key role in addressing climate change and implementing low-carbon economic strategies. Effectively promoting the implementation of regional carbon emission reduction policies in China is of paramount importance for achieving the "carbon peak and carbon neutrality" goals. Hence, a differential analysis of the emission characteristics and peak trends of the BTH and the YRD can provide valuable theoretical references and policy insights for advancing China's coordinated regional development and promoting environmental sustainability.

This paper makes several contributions. Firstly, from the research perspective, it extends the research scope of carbon peak from a single region to a comparison of regional differences in two major regions, the BTH and YRD; the two are analysed in comparison. Through this comparative perspective, the key issues and challenges faced by the two regions in the process of moving towards carbon peak are revealed, providing in-depth insights into regionally

differentiated carbon reduction strategies. Secondly, regarding the research content, carbon emissions from the BTH and YRD are estimated over the period spanning from 1990 to 2021 and their current characteristics are evaluated in comparison. Also, the differences in the influencing factors are examined after screening. This study forecasts the timing and magnitude of carbon peaks, enabling the formulation of tailored policy recommendations that provide strategic guidance for other regions aiming to realize the "carbon peak and carbon neutrality" targets and advance low-carbon development. Finally, regarding research methodology, the PSO-SVR model is integrated with dynamic scenario analysis to predict carbon peaking in the two regions. By employing the Monte Carlo simulation method to account for future uncertainties, dynamic scenario analysis is utilized to explore potential carbon emission trajectories under various development scenarios. Subsequently, the PSO-SVR model is applied to improve forecast accuracy, providing a robust methodological framework for precise carbon emission projections and informed policy decision-making.

2. Literature Review

Due to the country's emphasis on the "carbon peak and carbon neutrality" goals, numerous researches frequently concentrate on national-level carbon emissions, the provincial level (Qi. Wang *et al.*, 2016) and some even use individual prefecture-level cities (Z. H. Wang *et al.*, 2012) as examples. Z. H. Xie *et al.* (2021) analysed how technological advancements influence carbon emission efficiency across China as a whole. Dong and Li (2022a) selected Jiangsu province as the focal point of their study, predicting and comparing the carbon emission trends under five scenarios. Qin *et al.* (2024) examined carbon peaking predictions and carbon reduction pathways in low-carbon pilot cities, utilizing Wuxi as a case.

When examining the driver analysis models, Ehrlich and Holdren (1971) highlighted the role of population in environmental impacts through the introduction of the IPAT equation, which posits that *Impact* = *Population* × *Affluence* × *Technology*. However, Dietz and Rosa (1997) later pointed out that the IPAT equation constrained environmental research. Consequently, scholars proposed the STIRPAT model, which can better reflect the interrelationship between variables and the environment. As a result, the model gained widespread adoption in the exploration of factors influencing carbon emissions (Dietz and Rosa, 1997). Through the expanded STIRPAT model, R. Wu *et al.* (2021) examined the degree to which different driving factors affect CO_2 emissions. The STIRPAT model allows multiple impact analyses and the results are easy to interpret, making it suitable for analysing multiple impact factors in this study.

Regarding the driving factors and mechanisms, a large number of scholars generally believe that CO_2 emissions are influenced by a combination of factors, including economic growth, urbanization level, population size, industrial structure and energy intensity (X. Li *et al*., 2024; Quan *et al.*, 2020; Du *et al*., 2018). M. Liu *et al.* (2023) developed an innovative decomposition model that integrates input-output subsystem analysis with structural decomposition analysis. Their study reveals that while economic growth drives an increase in CO_2 emissions, energy intensity acts as a mitigating force. Similarly, Chong *et al.* (2019) employed the LMDI decomposition model to identify that the critical factors influencing CO_2 emissions are energy intensity, population growth and GDP per capita. Ma *et al.* (2019) employed the Kaya identity in conjunction with the LMDI model and demonstrated that industrial structure facilitates reductions in carbon intensity, whereas economic growth and population expansion hinder carbon emission reductions. Lv *et al.* (2019) concluded that urbanization positively affects CO_2 emissions by utilizing the GWR-STIRPAT model. Drawing on these studies, we select the five mentioned factors as the primary variables for our analysis.

In carbon emission forecasting, the grey model (Gao *et al.*, 2023; W. Zhou *et al.*, 2021) and the LEAP model (Hu *et al.*, 2019) are commonly used. With the advancement of machine learning, the use of predictive models based on machine learning has significantly increased. For instance, Sun and Liu (2016) used LSSVM algorithms for forecasting emissions in Hebei province, while Huang *et al.* (2019) demonstrated that LSTM networks outperform BPNN and GPR in predicting emissions in China. Scenario analysis is another common approach, as illustrated by Guo and Pang's (2023) expanded STIRPAT model for simulating carbon peaking across 31 provinces in China. Similarly, F. Ren and Long (2021) combined the Optimized Rapid Learning Network algorithm with static scenario analysis to examine the carbon peaking status in Guangdong province.

Currently, while many scholars have studied the impact mechanisms and carbon peaking predictions for the BTH and YRD regions (Zhu and Zhang, 2021; Cui *et al.*, 2024; C. Chen *et al.*, 2023; Zhan *et al.*, 2024; Y. Zhou *et al.*, 2021; J. Ren *et al.*, 2023; W. Wu *et al.*, 2021), there is a relative lack of differentiated peak prediction analysis focusing on the unique characteristics of carbon emissions in these regions. National-level studies fail to capture regional differences, and provincial-level studies are often too specific to be broadly applicable. Much of the existing literature combines machine learning algorithms with static scenario analysis, which fails to account for future uncertainties. In contrast, Monte Carlo simulation provides a dynamic and comprehensive approach to scenario analysis by simulating random parameter intervals. Among predictive models, the support vector regression (SVR) model, particularly when optimized with the particle swarm optimization (PSO) algorithm,

demonstrates exceptional performance in addressing nonlinearity, managing small sample sizes and handling high-dimensional data. This combination enhances prediction accuracy while mitigating the risk of overfitting. We aim to address gaps in predicting carbon emission differentiation and dynamic scenario setting for these two regions. We propose combining Monte Carlo simulation with the PSO-SVR model to provide a novel framework for forecasting carbon emission trends and supporting policy decisions.

3. Methods and Data

3.1 Estimation of CO_2 emissions

Since the statistical yearbook neither provides direct carbon dioxide data nor outlines a standard calculation method (Qu. Wang *et al.*, 2015), carbon dioxide estimates are commonly derived from data on major fossil fuels by most scholars (Donglan *et al.*, 2010). According to the assessment report by the IPCC (2007), burning of fossil fuels remains the foremost contributor to the rising greenhouse gas emissions, with coal, crude oil, coke, kerosene, gasoline, diesel, natural gas and fuel oil being the main sources responsible for emitting carbon dioxide. Based on the accounting method used by Shan *et al.* (2018), the consumption data for eight different types of energy in the provinces within the BTH and the YRD from 1990 to 2021 are utilized to calculate the CO_2 emissions. CO_2 emissions are accounted for as shown in Equation (1), where C represents carbon emissions, i denotes the type of energy source, E_i denotes its consumption and F_i stands for its CO_2 emission coefficient.

$$C = \sum_{i=1} E_i \times F_i \tag{1}$$

3.2 STIRPAT model

We adopt an expanded STIRPAT model to investigate the different factors that influence CO_2 emissions in both the BTH and the YRD. The STIRPAT model addresses the limitation of the IPAT model that "each factor has the same impact on environmental conditions" (York *et al.*, 2003). Equation (2) presents the linear logarithmic format of the STIRPAT model. I represents the environmental pressure indicator, a is the model coefficient and P stands for population, where b is the corresponding index. A signifies affluence, with c being the index of affluence. T denotes the technology level, d reflects the technological level index and ε represents the random error term.

$$\ln I = a + b\ln P + c\ln A + d\ln T + \varepsilon \tag{2}$$

The model can be extended appropriately. In this study, the regional characteristics of the BTH and the YRD are thus integrated, with a focus on five influential factors: population (*P*), energy intensity (*EI*), GDP per capita (*A*), industrial structure (*IS*) and urbanization rate (*U*). Substituting these five variables for the variables in Equation (2), we obtain the extended STIRPAT model by taking their logarithms as shown in Equation (3). Here, *t* represents time, P_t, A_t, EI_t, IS_t, U_t represent the five influencing factors of time *t*, *a* is the model coefficient and *b*, *c*, *d*, *j* and *h* denote the coefficients assigned to each explanatory variable, while ε_t signifies the random disturbance term at the time *t*.

$$\ln C_t = a + b\ln P_t + c\ln A_t + d\ln EI_t + g\ln IS_t + h\ln U_t + \varepsilon_t \tag{3}$$

3.3 Ridge regression model

As a regression improvement model, ridge regression is a statistical approach designed to improve linear regression by addressing the issue of multicollinearity. When features are highly correlated, the ordinary least squares (OLS) method may produce unstable parameter estimates. This instability can negatively affect the predictive performance of the model. Ridge regression resolves this issue by introducing a regularization term into the loss function, which constrains the size of regression coefficients, reducing the model sensitivity to noise and enhancing its generalization ability (McDonald, 2009). The loss function of ridge regression is expressed in Equation (4), where *n* represents the total number of samples, *m* denotes the number of features, y_i represents the target value of the *i*-th sample, x_{ij} refers to the *j*-th feature value of the *i*-th sample, θ_j corresponds to the weight of the *j*-th feature and λ is the regularization parameter.

$$L(\theta) = \sum_{i=1}^{n}\left(y_i - \sum_{j=1}^{m}\theta_j x_{ij}\right)^2 + \lambda\sum_{j=1}^{m}\theta_j^2 \tag{4}$$

Furthermore, the design matrix $\mathbf{X}$ is an $n \times m$ matrix, where each row corresponds to an individual sample and each column represents a distinct feature. Usually, a bias term with a value of 1 is added to the design matrix so that the model includes an intercept term. The parameter estimation of ridge regression can be achieved by minimizing the loss function. Since the loss function is quadratic, it can be solved directly by analytical methods. Specifically, the parameters of ridge regression can be calculated using Equation (5), where $\mathbf{X}$ stands for the design matrix, *y* represents the target value vector, λ is the regularization parameter and $\mathbf{I}$ is the identity matrix.

$$\theta = (\mathbf{X}^T X + \lambda\mathbf{I})^{-1}\mathbf{X}^T y \tag{5}$$

When performing multiple regression calculations, if there is a correlation between multiple independent variables, the coefficients in the model will lose their practical meaning. Thus, it is essential to perform a multicollinearity test on the logarithms of the independent variables in the STIRPAT model. As we can see in the results in table 1, the variance inflation factor (VIF) significantly exceeds 10. Furthermore, the tolerance is also below 0.1. These values show that there is serious multicollinearity between the variables. Hence, we adopt the ridge regression model to solve the multicollinearity problem.

Table 1: Multicollinearity test

Region	Variable	Tolerance	VIF	Region	Variable	Tolerance	VIF
BTH	ln*P*	0.019	52.619	**YRD**	ln*P*	0.012	82.048
	ln*A*	0.003	321.815		ln*A*	0.007	149.261
	ln*EI*	0.018	56.785		ln*EI*	0.007	153.523
	ln*IS*	0.020	50.773		ln*IS*	0.009	109.306
	ln*U*	0.014	69.403		ln*U*	0.044	22.751

Source: Authors' own calculations

3.4 PSO-SVR model

Cortes and Vapnik (1995) introduced the ε-insensitive loss function in SVM to create support vector regression (SVR), which addresses machine learning problems with limited samples and nonlinear features, offering a global optimal solution and efficient computation in high-dimensional data. The objective of the SVR model is to fit the data while selecting appropriate hyperparameters to minimize the loss function. Equation (6) shows the function expression of the SVR model; $f(x)$ is the predicted output of SVR for input x, b stands for the bias term, $\boldsymbol{x}$ represents the input feature vector and $\boldsymbol{w}$ represents the weight vector.

$$f(x) = \langle \boldsymbol{w}, \boldsymbol{x} \rangle + b \tag{6}$$

Introducing a slack variable ξ_i for each sample point (x_i, y_i) and penalty coefficients C into the above optimization problem, the objective function and its constraints are shown in Equations (7) and (8); y is the true target value, ε is the epsilon-insensitive parameter that defines a margin of tolerance where no penalty is given, ξ_i are slack variables that allow some flexibility in the model and C represents a regularization parameter that governs

the balance between the model complexity (minimizing $||w||^2$) and the penalty for violating the ε-insensitive loss.

$$\min_{w,b,\xi} \quad \frac{1}{2}\|w\|^2 + C\sum_{i=1}^{N}\xi_i \tag{7}$$

$$s.t.\ f(x_i) - y_i \le \epsilon + \xi_i,\ y_i - f(x_i) \le \epsilon + \xi_i,\ \xi_i \ge 0,\ i = 1, 2, \cdots, n \tag{8}$$

The dual form of the optimization problem is derived using Lagrange multipliers. The dual formulation allows us to solve the problem in terms of kernel functions, making SVR efficient in high-dimensional spaces. Considering the nonlinear mapping $\Phi(x)$ and the kernel function $K(x; z)$, it is easy to obtain the dual form of nonlinear support vector regression in Equation (9), where $K(x; x_i) = \Phi(x) \times \Phi(x_i)$, α_i; α_i^* is the solution to the dual form of the optimization problem.

$$f(x) = \sum_{i=1}^{n}(\alpha_i - \alpha_i^*)K(x, x_i) + b \tag{9}$$

Since the predicted output of SVR is easily affected by the hyperparameters of SVR (such as the penalty parameter c, ε and kernel function parameters γ), it is necessary to introduce particle swarm optimization (PSO) for searching the optimal hyperparameters. The PSO process updates the particle positions and velocities to search for the optimal hyperparameters. The velocity and position update equations are Equations (10) and (11). v_i^{t+1} represents the velocity of the particle i at the iteration $t + 1$. x_i^{t+1} denotes the position of the particle i at the same iteration (*i.e.*, the hyperparameter values such as c, ε and γ); w represents the inertia weight, governing the dependence of the particle on its previous velocity; r_1 and r_2 represent random values used to introduce randomness into the search process; c_1 and c_2 are learning factors (c_1 controls the particle dependence on its individual best position, while c_2 governs the particle reliance on the global best position); $pbest_i$ refers to the best position discovered by the particle i individually, while $gbest$ represents the best position identified by the entire swarm collectively (*i.e.*, the optimal hyperparameter values).

$$v_i^{t+1} = w \cdot v_i^t + c_1 \cdot r_1 \cdot (pbest_i - x_i^t) + c_2 \cdot r_2 \cdot (gbest - x_i^t) \tag{10}$$

$$x_i^{t+1} = x_i^t + v_i^{t+1} \tag{11}$$

To evaluate the accuracy and precision of the forecasting model, three distinct metrics are employed. The root mean square error (RMSE) measures the average magnitude of errors, the mean absolute percentage error (MAPE) quantifies prediction accuracy in percentage terms and the mean absolute error (MAE) calculates the average absolute differences

between predicted and observed values. The accuracy of the prediction model increases as the values of these three indicators decrease. The evaluation criteria formulas are presented in Equations (12), (13) and (14), where Y is the observed carbon emissions and $\widehat{Y}$ represents the model for predicting carbon emissions.

$$MAE = \frac{1}{n}\sum_{i=1}^{n} |Y_i - \widehat{Y_i}| \tag{12}$$

$$RMSE = \sqrt{\frac{\sum_{i=1}^{n}(Y_i - \widehat{Y_i})^2}{n}} \tag{13}$$

$$MAPE = \frac{1}{n}\sum_{i=1}^{n} \frac{|Y_i - \widehat{Y_i}|}{Y_i} \tag{14}$$

3.5 Data

We select P, A, U, IS and EI as explanatory variables, with C serving as the dependent variable. The data sample spans the years from 1990 to 2021. Table 2 provides a detailed description of these variables. The various energy consumption data used in this paper are sourced from the China Energy Statistical Yearbook (National Bureau of Statistics of China, 2022). Population, urbanization rate, GDP and industrial structure are acquired from the China Statistical Yearbook (National Bureau of Statistics of China, 2022). The GDP is converted to the base period with the constant price in 1990.

Table 2: Explanation of variables

Variables	Full name	Interpretations	Unit
C	Carbon emissions	CO_2 emissions	100 million tonnes
P	Population	Resident population	10,000 people
A	GDP per capital	Population per unit of GDP	10,000 yuan/person
EI	Energy intensity	Energy consumption per unit of GDP	tce / 10,000 yuan
IS	Industrial structure	Output value of tertiary industry per unit of GDP	%
U	Urbanization rate	Ratio of urban population to population	%

Source: Authors' own elaboration

3.6 Dynamic scenario setting

Increasing concerns about climate change have prompted scholars to employ diverse methods for forecasting future emissions (Gao *et al.*, 2023; Zhan *et al.*, 2024; Hu *et al.*, 2019). Lin and Ouyang (2014) argue that scenario analysis is superior in showing the impacts of different policies on carbon emission trajectories, making it valuable for policymakers. They suggest that developing three scenarios is optimal, as more can lead to unclear analysis. Thus, the following three scenarios are proposed for carbon emissions in two regions: a baseline scenario combining the 14th Five-Year Plan and previous growth rates, a low-carbon scenario with stronger environmental policies and green technology, and a high-carbon scenario focused on economic growth. Considering the uncertainties of influencing factors (Vithayasrichareon and MacGill, 2012), Monte Carlo simulation offers dynamic projections by incorporating risk analysis. By integrating scenario analysis with Monte Carlo simulation, we create a comprehensive framework for carbon emission trajectories. Applying a Monte Carlo simulation first requires providing the future change rates for each relevant variable as inputs, followed by randomly extracting from a predefined sample and then simulating the results of the extraction. Finally, in order to better display the maximum possible prediction value, we use a probability distribution diagram to present it. Since the future change rate of the input variable has a specific degree of certainty, a triangular distribution is selected for 100,000 simulations (Vithayasrichareon and MacGill, 2012). We set minimum values, median values and maximum values for the simulation. The maximum and minimum of the rate of change of each factor in the future are set with reference to the annual average maximum and minimum change rates calculated based on the data for the 13th Five-Year Plan period. At the same time, adjustments are made in accordance with the 14th Five-Year Plan. In the baseline scenario, the BTH and the YRD are set according to past development characteristics and the actual economic growth during the 14th Five-Year Plan. As a pivotal document issued by the Chinese government, the Five-Year Plan outlines the country's economic development strategy, establishes growth targets and offers guidance for reforms (Shiu and Lam, 2004). The anticipated impact of the Five-Year Plan is expected to manifest significantly in economic development, investment patterns and environmental pollution levels. Additionally, it is projected to positively influence environmental governance. Consequently, the elements are aligned with the national planning timeline.

Table 3: Average annual growth rates of influencing factors in baseline scenario (%)

		2022–2025			2026–2030			2031–2035		
Region	**Variable**	**Min**	**Median**	**Max**	**Min**	**Median**	**Max**	**Min**	**Median**	**Max**
BTH	***A***	4.7	5.2	5.7	4.2	4.7	5.2	3.7	4.2	4.7
	P	0.06	0.16	0.26	−0.14	−0.04	0.06	−0.34	−0.24	−0.14
	EI	−3.2	−2.7	−2.2	−2.7	−2.2	1.7	2.2	1.7	1.2
	U	1.31	1.51	1.71	1.11	1.31	1.51	0.91	1.11	1.31
YRD	***A***	5	5.5	6	4.5	5	5.5	4	4.5	5
	P	0.63	0.73	0.83	0.43	0.53	0.63	0.23	0.33	0.43
	EI	−3.2	−2.7	−2.2	−2.7	−2.2	−1.7	−2.2	−1.7	−1.2
	IS	1.46	1.66	1.86	1.26	1.46	1.66	1.06	1.26	1.46
	U	1.7	1.9	2.1	1.5	1.7	1.9	1.3	1.5	1.7

Source: Authors' own calculations

Both the BTH and the YRD have first-tier cities as their core, which can attract talents and generate population flows. The population is expected to experience a certain degree of growth in the short term. Consequently, the median values for the average annual population growth rates for the period 2022–2025 are established at 0.16% and 0.73% in the BTH and the YRD, respectively. The changes in subsequent years and the other two scenarios refer to the settings and forecasts of population in Y. Chen *et al*. (2020). Since China's economic activities have been affected to some extent by COVID-19 (Q. Li *et al*., 2024), the median values for GDP per capita for 2022–2025 are set at 5.2% and 5.5% in the BTH and the YRD, respectively. Other settings refer to J. Zhou *et al.* (2018). The other two scenarios for the two regions fluctuate by 0.5 percentage points (Wen and Liu, 2016). According to China's 14th Five-Year Plan, energy intensity is projected to decline by 13.5% by 2025. Following this plan, the median values for energy intensity in both regions are set at −2.7%. The urbanization rates of both regions and the industrial structure of the YRD are set in accordance with the average annual growth rates recorded throughout the 13th Five-Year Plan period. This setting is made while considering the actual economic development in these regions. According to X. Zhang *et al.* (2020), the variation ranges are usually 0.3–0.5 percentage points for the change rates of energy intensity, on the basis of the middle level. Therefore, we set the energy intensity for the two other scenarios to fluctuate by 0.5%. The urbanization rate in both regions and the industrial structure of the YRD fluctuate by 0.2% (P. Xie *et al.*, 2022; Y. Chen *et al*., 2020). Tables 3, 4 and 5 illustrate the settings in detail.

Table 4: Average annual growth rates of influencing factors in low-carbon scenario (%)

		2022–2025			2026–2030			2031–2035		
Region	**Variable**	**Min**	**Median**	**Max**	**Min**	**Median**	**Max**	**Min**	**Median**	**Max**
BTH	***A***	4.2	4.7	5.2	3.7	4.2	4.7	3.2	3.7	4.2
	P	0.01	0.11	0.21	−0.19	−0.09	0.01	−0.39	−0.29	0.19
	EI	−4.2	−3.7	−3.2	−3.7	−3.2	−2.7	−3.2	−2.7	−2.2
	U	1.11	1.31	1.51	0.91	1.11	1.31	0.71	0.91	1.11
YRD	***A***	4.5	5	5.5	4	4.5	5	3.5	4	4.5
	P	0.43	0.53	0.63	0.23	0.33	0.43	0.03	0.13	0.23
	EI	−4.2	−3.7	−3.2	−3.7	−3.2	−2.7	−3.2	−2.7	−2.2
	IS	1.66	1.86	2.06	1.46	1.66	1.86	1.26	1.46	1.66
	U	1.5	1.7	1.9	1.3	1.5	1.7	1.1	1.3	1.5

Source: Authors' own calculations

Table 5: Average annual growth rates of influencing factors in high-carbon scenario (%)

		2022–2025			2026–2030			2031–2035		
Region	**Variable**	**Min**	**Median**	**Max**	**Min**	**Median**	**Max**	**Min**	**Median**	**Max**
BTH	***A***	5.2	5.7	6.2	4.7	5.2	5.7	4.2	4.7	5.2
	P	0.11	0.21	0.31	−0.09	0.01	0.11	−0.29	−0.19	−0.09
	EI	−2.2	−1.7	−1.2	−1.7	−1.2	−0.7	−1.2	−0.7	−0.2
	U	1.51	1.71	1.91	1.31	1.51	1.71	1.11	1.31	1.51
YRD	***A***	5.5	6	6.5	5	5.5	6	4.5	5	5.5
	P	0.83	0.93	1.03	0.63	0.73	0.83	0.43	0.53	0.63
	EI	−2.2	−1.7	−1.2	−1.7	−1.2	−0.7	−1.2	−0.7	−0.2
	IS	1.26	1.46	1.66	1.06	1.26	1.46	0.86	1.06	1.26
	U	1.9	2.1	2.3	1.7	1.9	2.1	1.5	1.7	1.9

Source: Authors' own calculations

4. Results

4.1 Analysis of current CO_2 emission situation

In order to explore the similarities and differences between the CO_2 emissions in the BTH and the YRD, we add the change in carbon emission intensity (CI) for analysis (J. Liu *et al*., 2021). Figure 1 shows the changes in CO_2 emissions and CI in the BTH and the YRD from 1990 to 2021. During this period, the CI of the two regions generally showed a downward trend. It indicates that the CO_2 emission growth rate in the two regions lagged behind the economic growth rate over the same period. The CO_2 emissions in the two regions generally showed an upward trend. This results from rapid economic growth and the increase in manufacturing industries, which further expanded the demand for fossil fuels, leading to a rise in CO_2 emissions in the two regions (Dong and Li, 2022b). It is evident that CO_2 emissions in the BTH are lower than those in the YRD. However, the CI of the BTH is significantly higher, while that of the YRD is lower. Over the long term, CO_2 emissions in the BTH are primarily influenced by CO_2 emissions from Hebei, which has primarily relied on heavy industry and energy-intensive sectors, resulting in high levels of carbon emission intensity (W. Li *et al.*, 2018). In contrast, the YRD has a more diversified economy with a larger proportion of services and high-tech industries, which typically have lower carbon intensity (J. Wu *et al.*, 2018). The YRD has relatively higher energy efficiency. In particular, there is a greater level of clean energy adoption and advanced production technologies in industrial and transportation sectors. While the BTH is also making progress in green transformation, it still relies on many high-pollution, energy-intensive industries (Cheng *et al.*, 2018). This makes energy use efficiency relatively low. Similarly, the CI of both regions increased between 2002 and 2005. During the period 2002-2005, the main goal of national policy was to promote economic development, with relatively less attention paid to environmental protection and emission reduction (K. M. Zhang *et al.*, 2008). Therefore, the regions did not implement strict control measures on carbon emissions while promoting economic growth.

Figure 1: Comparison of CO_2 emission situation in BTH and YRD

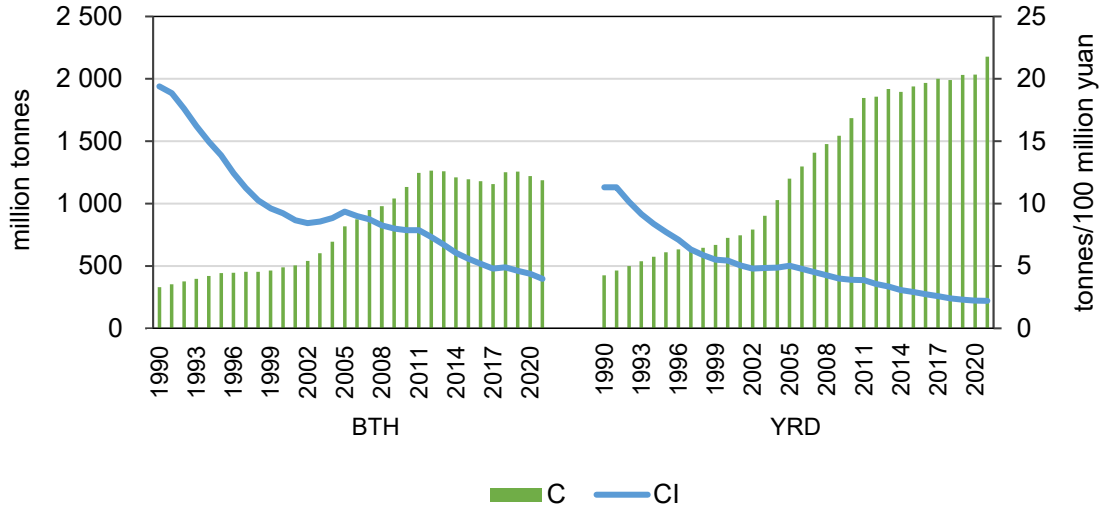

Source: Authors' own elaboration

4.2 Analysis of determinants affecting carbon emissions

To address multicollinearity, we use ridge regression. The ridge trace plot shows the optimal parameter k = 0.03 for both the BTH and YRD. Table 6 presents the results, with R^2 values of 98.11% for the BTH and 98.54% for the YRD, indicating a good fit. In the BTH, the p-values for ln$P$, ln$A$, lnEI and ln$U$ are all below 1%, confirming their significance, though lnIS is not significant. The F-test value for the BTH is 270.2786. In the YRD, the p-values for ln$P$, ln$A$, ln$U$ and lnIS are also below 1% and lnEI is significant at the 5% level. The F-test value for the YRD is 351.1649, confirming the significance of the model.

Table 6: Ridge regression results

Region	Variable	B	SE(B)	Beta	*t*	Sig.
BTH	ln*P*	2.0719	0.2871	0.4611	7.2163	0.0000
	ln*A*	0.2172	0.0232	0.3502	9.3578	0.0000
	ln*EI*	0.3363	0.0784	0.2605	4.2899	0.0002
	ln*IS*	0.0207	0.1507	0.0088	0.1372	0.8920
	ln*U*	0.5780	0.0854	0.4077	6.7715	0.0000
	constant	−19.6492	2.3920	0.0000	−8.2145	0.0000
YRD	ln*P*	2.6999	0.3449	0.4270	7.8275	0.0000
	ln*A*	0.3144	0.0279	0.5272	11.2605	0.0000
	ln*EI*	0.1231	0.0596	0.0945	2.0648	0.0490
	ln*IS*	−0.4250	0.1487	−0.1454	−2.8593	0.0083
	ln*U*	0.3629	0.0799	0.2622	4.5432	0.0001
	constant	−24.3359	3.1846	0.0000	−7.6418	0.0000

Note: BTH (F = 270.2786, R^2 = 0.9811, sig (F) = 0.0000); YRD (F = 351.1649, R^2 = 0.9854, sig (F) = 0.0000).
Source: Authors' own calculations

The regression results show that CO_2 emissions are propelled by urbanization, population growth and GDP per capita in the BTH and the YRD, while decreasing energy intensity and optimizing industrial structure reduce them. The impacts of these five drivers on CO_2 emissions are analysed individually.

In both the BTH and YRD, population growth is the main driver of CO_2 emissions. A 1% rise in population leads to a 2.07% increase in emissions in the BTH and a 2.70% increase in the YRD. This is due to the influx of people into central cities, causing uneven population distribution and rising demand, which increases energy consumption and CO_2 emissions. The same reason also leads to growing urbanization. Urbanization significantly affects carbon emissions. In the BTH, a 1% increase in urbanization raises emissions by 0.59%, while in the YRD, the increase is 0.36%. Urbanization has a stronger effect in the BTH due to accelerated urban construction and rising consumption, while in the YRD, its impact is smaller. In both regions, GDP per capita is positively correlated with emissions. However, its influence is relatively small compared to other factors. Rising GDP per capita typically indicates

higher levels of production and consumption, which often increases energy demand. Greater energy consumption leads to higher carbon emissions. Although GDP per capita contributes to increasing carbon emissions, the influence of other factors may directly reduce emissions, thereby diminishing the influence of GDP per capita.

The effect of the industrial structure on CO_2 emissions is insignificant in the BTH, likely due to differing dominant industries in Beijing, Tianjin and Hebei. In contrast, in the YRD, a 1% increase in the output value of tertiary industry reduces CO_2 emissions by 0.43%. Despite a shift from secondary to tertiary industry in the YRD, secondary industry remains significant, so further boosting the tertiary sector will help reduce emissions. In the BTH, a 1% rise in energy intensity leads to a 0.34% rise in CO_2 emissions, while it causes a 0.12% increase in the YRD. Energy intensity exerts a more significant influence on CO_2 emissions in the BTH. The YRD has been implementing energy efficiency improvements and low-carbon technologies more aggressively, partly due to stricter environmental regulations. This has helped lower its dependence on energy-intensive processes, reducing the impact of increases in energy intensity on CO_2 emissions. In contrast, while the BTH region is also making strides in energy efficiency, there is still potential for further improvement, resulting in a stronger relationship between energy intensity and CO_2 emissions. Technological improvements can reduce energy intensity and emissions, but more investment in research and development is needed. For the BTH, balancing energy, economic and environmental development is crucial, while reducing energy intensity remains an effective strategy for both regions. Advancing energy-saving technologies is key to further reducing emissions.

4.3 Analysis of carbon peaking prediction outcomes

In this paper, 75% of carbon emissions from both regions between 1990 and 2021 were chosen as the training samples and 25% as the test samples to assess the applicability and accuracy of the model. The test set results for the BTH showed MAE = 0.2426, RMSE = 0.2943 and MAPE = 3.6624%. The results of the test set for the YRD showed MAE = 0.4253, RMSE = 0.4966 and MAPE = 4.7046%. To accurately assess the prediction models, the predictive accuracy of the SVR model is evaluated in comparison with the PSO-SVR model (refer to figures 2 and 3). The PSO-SVR model yields smaller errors for both the BTH and the YRD compared to the SVR model, demonstrating its superior predictive accuracy. The MAPE value is less than 10%, indicating that it effectively forecasts the general trend of carbon emissions in both regions and maintains relatively stable relative prediction errors. This indicates its potential applicability for subsequent carbon emission predictions.

Figure 2: Error map of BTH

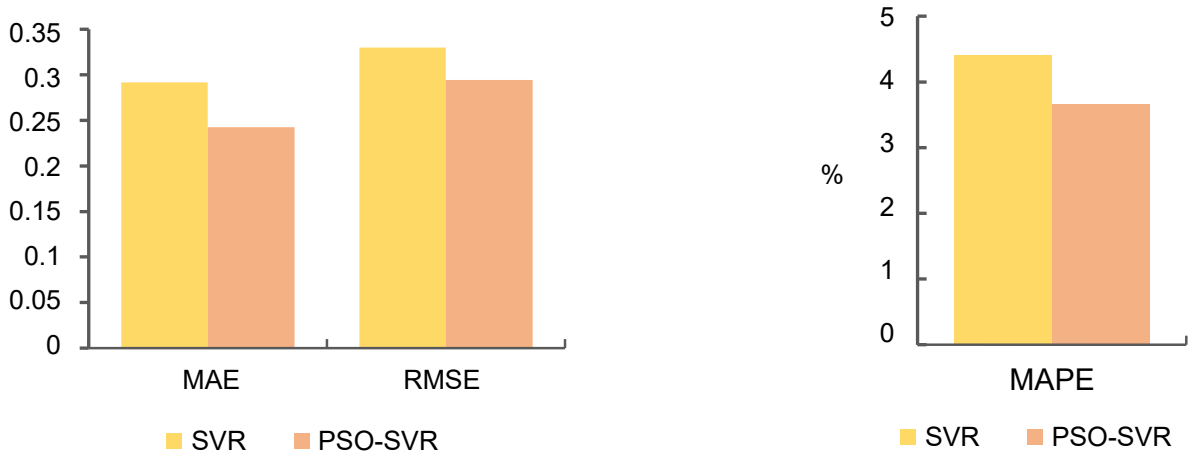

Source: Authors' own elaboration

Figure 3: Error map of YRD

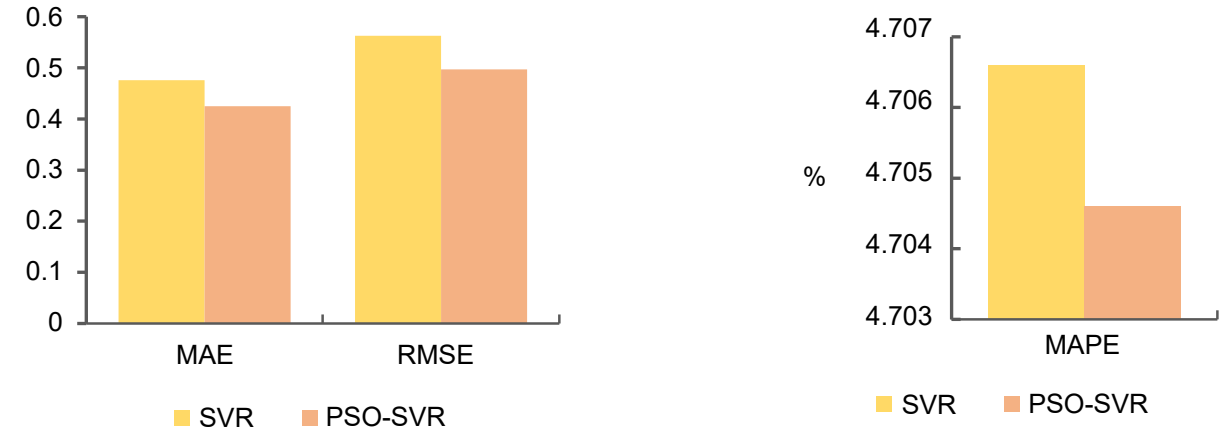

Source: Authors' own elaboration

We illustrate the future carbon emission trends of the BTH and the YRD under three scenarios. Under the baseline scenario, figure 4 shows that CO_2 emissions in the BTH will grow slowly until 2026 and then may decline. However, CO_2 emissions in the YRD will grow rapidly until 2025 and may not decline until 2028. As a result, carbon peak occurs later in the YRD than in the BTH. In 2026, the BTH has the highest probability of occurring at 1,202.95 million tonnes, while in 2028, the YRD has the highest probability of occurring at 2,310.75 million tonnes. CO_2 emissions in the BTH rise by 1.41% and in the YRD by 6.15% from 2021 to 2026. If the current growth and emission trends are maintained, the BTH and the YRD are expect-

ed to reach their carbon peaks before 2030. Hence, it is imperative for the government and relevant authorities to proactively devise emission reduction policies, advance green and sustainable development in both regions and encourage enterprises to voluntarily reduce carbon emissions. Additionally, effectively regulating the carbon emissions of enterprises can safeguard the achievement of carbon reduction targets.

In the low-carbon scenario, as shown in figure 5, the situation of the decrease in CO_2 emissions in the BTH begins to occur in 2022, when the probability of carbon emissions occurring at 1,192.18 million tonnes is the highest in the BTH. In contrast, carbon emissions in the YRD begin to decline in 2027, with the highest probability of occurring at 2,252.8 million tonnes. In general, a reasonable and effective investment of more funds and technologies in low-carbon production can greatly improve energy intensity and increase the efficiency of economic and industrial development. Ultimately, it will help the two regions achieve the national carbon peaking plan ahead of schedule and will also offer feasible solutions for achieving high-quality development. In the high-carbon scenario, as shown in Figure 6, the BTH exhibits the highest likelihood of carbon emissions decreasing after 2027, with an estimated occurrence at 1,230.08 million tonnes. The YRD has the highest probability of carbon emissions declining after 2029 and occurring at 2,365.87 million tonnes. Therefore, the high-carbon scenario has a higher value of carbon emissions although it also achieves peak carbon emissions by 2030. Both regions experience economic and carbon emission growth that has irreparable ecological impacts.

Scenario prediction analysis indicates that under the baseline model, both the BTH and YRD regions may achieve carbon peaking by 2030. However, the peak levels differ significantly. The primary factors influencing carbon peaks also vary between the two regions. As key national demonstration zones, the BTH and YRD will accelerate the country's path to carbon neutrality by peaking earlier. To ensure the success of emission reduction goals, efforts should address common challenges in both regions while considering regional differences and adopting tailored reduction strategies.

Figure 4: Carbon emission outcomes of baseline scenarios in BTH and YRD

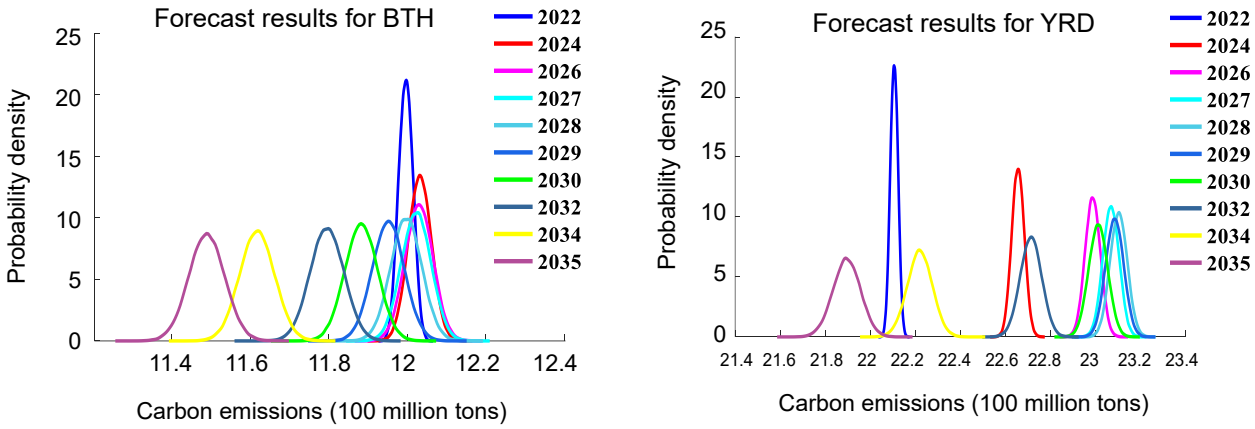

Source: Authors' own elaboration

Figure 5: Carbon emission outcomes of low-carbon scenarios in BTH and YRD

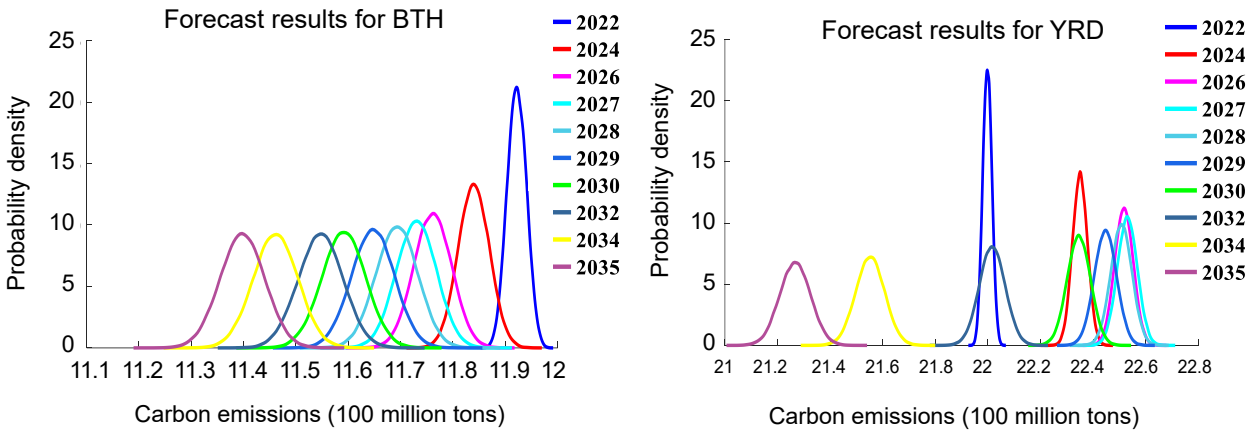

Source: Authors' own elaboration

Figure 6: Carbon emission outcomes of high-carbon scenarios in BTH and YRD

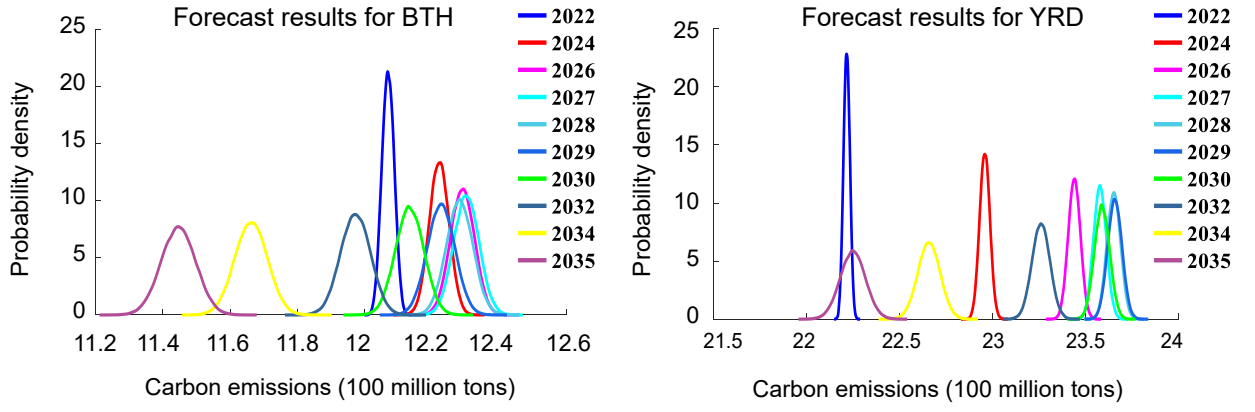

Source: Authors' own elaboration

5. Discussion

5.1 Common path in synergistic carbon reduction

In both the BTH and the YRD, variations exist in the levels of development among the provinces and municipalities within each region. To achieve an early carbon peak for the region as a whole, collaborative development and joint implementation of carbon reduction measures are necessary. Policy synergy and innovation mechanisms are the keys to a synergistic development of the two regions. Different provinces and cities have different government departments and adopt different energy-saving and carbon reduction policies; this has led to a lack of coordination mechanisms among government departments to manage carbon reduction and emission reduction. To solve the problems that have arisen, government departments in various regions have strengthened the coordination and integration of pollution control and emission reduction efforts across regulatory standards, management systems and market mechanisms. The carbon emission management system of local governments at all levels of division of labour and cooperation will achieve the carbon peak targets in both regions ahead of schedule under the joint effect of the benefit-sharing coordination mechanism, the linkage and long-term mechanism, the carbon emission assessment mechanism, the carbon emission reduction compensation mechanism and the supervision mechanism.

5.2 Energy-saving and carbon reduction pathway in BTH focuses on achieving decarbonization of energy

Compared with the YRD, the BTH has a more significant emission reduction effect brought by reducing energy intensity. With abundant renewable resources, the BTH should vigorously utilize these resources to implement coal substitution. Additionally, efforts should focus on improving recycling and low-carbon production technologies while encouraging the growth of clean energy sources. This will gradually replace coal with clean energy in the vacated space. Hebei province has substantial potential and opportunities to develop renewable energy within the BTH. However, the current industrial structure, dominated by manufacturing, does not have enough capacity to accommodate renewable energy. Beijing and Tianjin, on the other hand, have sufficient capital and technology to use the industrial advantages of renewable energy. Therefore, strengthening the BTH synergy is conducive to complementing each other's strengths, increasing the adoption of clean energy and facilitating optimal large-scale, cross-provincial and cross-city allocation of renewable and low-carbon energy resources.

5.3 Industrial system transformation path towards modernization and development with low carbon in YRD

At present, in the YRD, the manufacturing industry still presents the industrial structure of "too much low-end and too little high-end". This imbalance has contributed to the growing regional carbon emissions, signalling an urgent need for modernization and advancement of traditional industries in the YRD. An initial step in the low-carbon transformation of the YRD involves robustly implementing industrial digitalization and exploiting technologies such as artificial intelligence, the internet and big data to enhance industrial processes. A new form of "internet + manufacturing" will be formed. By embracing digital transformation, we can propel the intelligent evolution and modernization of traditional industries. Secondly, it is essential to use the regional advantages of the YRD and create unique industrial clusters. The development plan, which has been approved by the State Council, indicates that the YRD has unique advantages in promoting the development of industrial cluster chains. However, the task of "replenishing, fixing and strengthening the chain" of key industries is still arduous. Some highly externally oriented enterprises in the YRD rely on overseas markets for upstream raw materials and intermediate goods supply. If an accident occurs, it is easy for the industry chain to break, so it is necessary for the industry to seek import substitution to make up for the chain. As for the situation of identical industrial layout and homogeneous and vicious competition, it is necessary for the YRD to optimize the layout of the industry chain, integrate the provinces in the region into a chain and break the geographic constraints to consider the industrial division of labour throughout the region. It is necessary to make the industry chain stronger. The key to strengthening the industry chain lies in the development of core technologies. The YRD should make every effort to build an industry chain with key core technologies and science and technology R&D platform enterprises, so as to prompt the low-end and middle-end industries to move towards high-end industries. Finally, the YRD needs to support strategic emerging industries, especially those with strong digital economy attributes, including blockchain, biomedicine, artificial intelligence, integrated circuits and science and technology finance.

6. Conclusion and Implications

Using CO_2 emission data from 1990 to 2021, we adopted the expanded STIRPAT model to examine the drivers contributing to CO_2 emission disparities between the BTH and YRD regions and used ridge regression to further explore these differences. Three scenarios – baseline, low-carbon and high-carbon – were employed to forecast the timing and peaks of CO_2 emissions using the PSO-SVR model and Monte Carlo simulation. The results indicate that

population, energy intensity, urbanization and GDP per capita significantly influence emissions in both regions, with industrial structure affecting only the YRD. Population is the primary driver in both regions. In the BTH, energy intensity has a stronger effect, while urbanization affects the YRD more. The baseline scenario predicts carbon peaks in 2026 for the BTH (1,202.95 million tonnes) and 2028 for the YRD (2,310.75 million tonnes). In the low-carbon scenario, peaks occur in 2022 for the BTH (1,192.18 million tonnes) and 2027 for the YRD (2,252.8 million tonnes). The peaks are delayed to 2027 and 2029 in the high-carbon scenario, with respective emissions of 1,230.08 million tonnes for the BTH and 2,365.87 million tonnes for the YRD.

Based on the above conclusions, the government should adopt a tailored approach to emission reduction policies, considering the different carbon peaking scenarios in the BTH and YRD regions to meet their unique environmental and economic needs. For the BTH, with high carbon emission intensity, the focus should be on industrial transformation, upgrading and adjusting the energy structure. Stricter policies are needed to achieve carbon peaking as soon as possible. In contrast, the YRD should prioritize developing the service and high-tech industries, and enhancing cooperation in carbon control to ensure a gradual emissions decline and a progressive peak. Additionally, both regions should strengthen mutual collaboration, promote complementary advantages and share resources to advance the carbon peaking process.

However, there are still some limitations. Firstly, we considered only eight major energy sources in the carbon emission accounting. Considering more energy sources will help improve the accuracy of carbon emission accounting. Secondly, our selection of influencing factors was limited, and more influencing factors are not comprehensively considered, which to a certain extent will affect the selection of subsequent predictor variables and prediction results. Moreover, this study focused solely on the provincial level, excluding city-level analysis. Future research could explore carbon emission predictions and influencing factor analyses using more granular urban data, providing deeper insights into the disparities in carbon emissions across regions and units of varying sizes. Finally, we carried out only an error comparison of two algorithms in making the selection of machine learning algorithms. In the future, more machine learning algorithms can be considered to improve the prediction accuracy.

Acknowledgement

Conflict of interest statement: The authors hereby declare that this article was neither submitted nor published elsewhere and they have no competing interests.

Funding: This research was funded by the National Social Science Fund of China (22CJY060); Hainan Provincial Natural Science Foundation of China (724RC497); Hainan Provincial "The South China Sea Rising Star" Philosophy and Social Science Talent Platform Project (HNSKL-NHXX202501).

AI usage statement: The authors confirm that no artificial intelligence (AI) or AI-assisted tools were used in the creation of this manuscript.

Availability of data and materials: Data will be made available on request.

Authors' contributions: Yang Yu: conceptualization, investigation, methodology, project administration, writing – original draft. Yaping Gong: data curation, software, supervision, validation, visualization, writing – review and editing. Doohwan Won: visualization, writing – review and editing. Atif Jahanger: resources, validation.

References

Chen, C., Luo, Y., Zou, H., et al. (2023). Understanding the driving factors and finding the pathway to mitigating carbon emissions in China's Yangtze River Delta region. *Energy*, 278(B), 127897. https://doi.org/10.1016/j.energy.2023.127897

Chen, Y., Guo, F., Wang, J., et al. (2020). Provincial and gridded population projection for China under shared socioeconomic pathways from 2010 to 2100. *Scientific Data*, 7(1), 83. https://doi.org/10.1038/s41597-020-0421-y

Cheng, X., Fan, L., Wang, J. (2018). Can energy structure optimization, industrial structure changes, technological improvements, and central and local governance effectively reduce atmospheric pollution in the Beijing-Tianjin-Hebei area in China? *Sustainability*, 10(3), 644. https://doi.org/10.3390/su10030644

Chong, C. H., Tan, W. X., Ting, Z. J., et al. (2019). The driving factors of energy-related CO_2 emission growth in Malaysia: The LMDI decomposition method based on energy allocation analysis. *Renewable and Sustainable Energy Reviews*, 115, 109356. https://doi.org/10.1016/j.rser.2019.109356

Cui, L., Wang, J., Chen, X., et al. (2024). Regional policy options for carbon peaking in the Yangtze River Delta under uncertainty. *Journal of Environmental Management*, 364, 121445. https://doi.org/10.1016/j.jenvman.2024.121445

Dietz, T., Rosa, E. A. (1997). Effects of population and affluence on CO_2 emissions. *Proceedings of the National Academy of Sciences*, 94(1), 175–179. https://doi.org/10.1073/pnas.94.1.175

Dong, J., Li, C. (2022a). Scenario prediction and decoupling analysis of carbon emission in Jiangsu Province, China. *Technological Forecasting and Social Change*, 185, 122074. https://doi.org/10.1016/j.techfore.2022.122074

Dong, J., Li, C. (2022b). Structure characteristics and influencing factors of China's carbon emission spatial correlation network: A study based on the dimension of urban agglomerations. *Science of the Total Environment,* 853, 158613. https://doi.org/10.1016/j.scitotenv.2022.158613

Donglan, Z., Dequn, Z., Peng, Z. (2010). Driving forces of residential CO_2 emissions in urban and rural China: An index decomposition analysis. *Energy policy*, 38(7), 3377–3383. https://doi.org/10.1016/j.enpol.2010.02.011

Du, G., Sun, C., Ouyang, X., et al. (2018). A decomposition analysis of energy-related CO_2 emissions in Chinese six high-energy intensive industries. *Journal of Cleaner Production*, 184, 1102–1112. https://doi.org/10.1016/j.jclepro.2018.02.304

Ehrlich, P. R., Holdren, J. P. (1971). Impact of Population Growth: Complacency concerning this component of man's predicament is unjustified and counterproductive. *Science*, 171(3977), 1212–1217. https://doi.org/10.1126/science.171.3977.1212

Gao, H., Wang, X., Wu, K., et al. (2023). A review of building carbon emission accounting and prediction models. *Buildings*, 13(7), 1617. https://doi.org/10.3390/buildings13071617

Guo, X., Pang, J. (2023). Analysis of provincial CO_2 emission peaking in China: Insights from production and consumption. *Applied Energy*, 331, 120446. https://doi.org/10.1016/j.apenergy.2022.120446

Hu, G., Ma, X., Ji, J. (2019). Scenarios and policies for sustainable urban energy development based on LEAP model–A case study of a postindustrial city: Shenzhen China. *Applied Energy*, 238, 876–886. https://doi.org/10.1016/j.apenergy.2019.01.162

Huang, Y., Shen, L., Liu, H. (2019). Grey relational analysis, principal component analysis and forecasting of carbon emissions based on long short-term memory in China. *Journal of Cleaner Production*, 209, 415–423. https://doi.org/10.1016/j.jclepro.2018.10.128

IPCC (2007). *Climate Change 2007: Mitigation of Climate Change*. Contribution of Working Groups I, II and III to the Fourth Assessment Report of the Intergovernmental Panel on Climate Change. Geneva: Intergovernmental Panel on Climate Change. Available at: https://www.ipcc.ch/report/ar4/wg3/

Li, Q., Yuan, Z., Tao, R. (2024). The political economy of COVID-19 in China. *China Economic Review*, 85, 102143. https://doi.org/10.1016/j.chieco.2024.102143

Li, W., An, C., Lu, C. (2018). The assessment framework of provincial carbon emission driving factors: an empirical analysis of Hebei Province. *Science of the total environment*, 637, 91–103. https://doi.org/10.1016/j.scitotenv.2018.04.419

Li, X., Lin, C., Lin, M., et al. (2024). Drivers, scenario prediction and policy simulation of the carbon emission system in Fujian Province (China). *Journal of Cleaner Production*, 434, 140375. https://doi.org/10.1016/j.jclepro.2023.140375

Lin, B. Q., Ouyang, X. L. (2014). Analysis of energy-related CO_2 (carbon dioxide) emissions and reduction potential in the Chinese non-metallic mineral products industry. *Energy*, 68, 688–697. https://doi.org/10.1016/j.energy.2014.01.069

Liu, J., Li, S., Ji, Q. (2021). Regional differences and driving factors analysis of carbon emission intensity from transport sector in China. *Energy*, 224, 120178. https://doi.org/10.1016/j.energy.2021.120178

Liu, M., Yang, X., Wen, J., et al. (2023). Drivers of Chinas carbon dioxide emissions: Based on the combination model of structural decomposition analysis and input-output subsystem method. *Environmental Impact Assessment Review*, 100, 107043. https://doi.org/10.1016/j.eiar.2023.107043

Lv, Q., Liu, H., Yang, D., et al. (2019). Effects of urbanization on freight transport carbon emissions in China: Common characteristics and regional disparity. *Journal of Cleaner Production*, 211, 481489. https://doi.org/10.1016/j.jclepro.2018.11.182

Ma, X., Wang, C., Dong, B., et al. (2019). Carbon emissions from energy consumption in China: Its measurement and driving factors. *Science of the Total Environment*, 648, 1411–1420. https://doi.org/10.1016/j.scitotenv.2018.08.183

McDonald, G. C. (2009). Ridge regression. *Wiley Interdisciplinary Reviews: Computational Statistics*, 1(1), 93–100. https://doi.org/10.1002/wics.14

National Bureau of Statistics of China (2022). *China Energy Statistical Yearbook*. [Retrieved 2024-11-14] Available at: https://data.cnki.net/yearBook/single?id=N2023050100&pinyinCode=YCXME

National Bureau of Statistics of China (2022). *China Statistical Yearbook*. [Retrieved 2024-11-14] Available at: https://www.stats.gov.cn/sj/ndsj/2022/indexch.htm

Qin, X. H., Xu, X. Y., Yang, Q. K. (2024). Carbon peak prediction and emission reduction pathways of China's low-carbon pilot cities: A case study of Wuxi city in Jiangsu province. *Journal of Cleaner Production*, 447. https://doi.org/10.1016/j.jclepro.2024.141385

Quan, C., Cheng, X., Yu, S., et al. (2020). Analysis on the influencing factors of carbon emission in China's logistics industry based on LMDI method. *Science of the Total Environment*, 734, 138473. https://doi.org/10.1016/j.scitotenv.2020.138473

Ren, F., Long, D. H. (2021). Carbon emission forecasting and scenario analysis in Guangdong Province based on optimized Fast Learning Network. *Journal of Cleaner Production*, 317. https://doi.org/10.1016/j.jclepro.2021.128408

Ren, J., Bai, H., Zhong, S. C., et al. (2023). Prediction of CO_2 emission peak and reduction potential of Beijing-Tianjin-Hebei urban agglomeration. *Journal of Cleaner Production*, 425. https://doi.org/ARTN13894510.1016/j.jclepro.2023.138945

Shan, Y., Guan, D., Zheng, H., et al. (2018). China CO_2 emission accounts 1997–2015. *Scientific data*, 5(1), 1–14. https://doi.org/10.1038/sdata.2017.201

Shi, Q. W., Liang, Q. Q., Huo, T. F., et al. (2023). Evaluation of CO_2 and SO2 synergistic emission reduction: The case of China. *Journal of Cleaner Production*, 433. https://doi.org/10.1016/j.jclepro.2023.139784

Shiu, A., Lam, P.-L. (2004). Electricity consumption and economic growth in China. *Energy Policy*, 32(1), 47–54. https://doi.org/10.1016/S0301-4215(02)00250-1

Sun, W., Liu, M. H. (2016). Prediction and analysis of the three major industries and residential consumption CO_2 emissions based on least squares support vector machine in China. *Journal of Cleaner Production*, 122, 144–153. https://doi.org/10.1016/j.jclepro.2016.02.053

Vithayasrichareon, P., MacGill, I. F. (2012). A Monte Carlo based decision-support tool for assessing generation portfolios in future carbon constrained electricity industries. *Energy Policy*, 41, 374–392. https://doi.org/10.1016/j.enpol.2011.10.060

Wang, H. K., Lu, X., Deng, Y., et al. (2019). China's CO_2 peak before 2030 implied from characteristics and growth of cities. *Nature Sustainability*, 2(8), 748–754. https://doi.org/10.1038/s41893-019-0339-6

Wang, Qu., Chiu, Y. H., Chiu, C. R. (2015). Driving factors behind carbon dioxide emissions in China: A modified production-theoretical decomposition analysis. *Energy Economics*, 51, 252–260. https://doi.org/10.1016/j.eneco.2015.07.009

Wang, Qi., Wu, S. D., Zeng, Y. E., et al. (2016). Exploring the relationship between urbanization, energy consumption, and CO_2 emissions in different provinces of China. *Renewable & Sustainable Energy Reviews*, 54, 1563–1579. https://doi.org/10.1016/j.rser.2015.10.090

Wang, Z. H., Yin, F. C., Zhang, Y. X., et al. (2012). An empirical research on the influencing factors of regional CO_2 emissions: Evidence from Beijing city, China. *Applied Energy*, 100, 277–284. https://doi.org/10.1016/j.apenergy.2012.05.038

Wei, M., Cai, Z., Song, Y., et al. (2024). Spatiotemporal evolutionary characteristics and driving forces of carbon emissions in three Chinese urban agglomerations. *Sustainable Cities and Society*, 104, 105320. https://doi.org/10.1016/j.scs.2024.105320

Wei, Y. M., Chen, K., Kang, J. N., et al. (2022). Policy and management of carbon peaking and carbon neutrality: A literature review. *Engineering*, 14, 52–63. https://doi.org/10.1016/j.eng.2021.12.018

Wen, L., Liu, Y. (2016). The Peak Value of Carbon Emissions in the Beijing-Tianjin-Hebei Region Based on the STIRPAT Model and Scenario Design. *Polish Journal of Environmental Studies*, 25(2), 823–834. https://doi.org/10.15244/pjoes/61244

Wu, J., Wei, Y. D., Li, Q., et al. (2018). Economic transition and changing location of manufacturing industry in China: A study of the Yangtze River Delta. *Sustainability*, 10(8), 2624. https://doi.org/10.3390/su10082624

Wu, R., Wang, J. Y., Wang, S. J., et al. (2021). The drivers of declining CO_2 emissions trends in developed nations using an extended STIRPAT model: A historical and prospective analysis. *Renewable & Sustainable Energy Reviews*, 149. https://doi.org/10.1016/j.rser.2021.111328

Wu, W., Zhang, T., Xie, X., et al. (2021). Regional low carbon development pathways for the Yangtze River Delta region in China. *Energy Policy*, 151, 112172. https://doi.org/10.1016/j.enpol.2021.112172

Xie, P., Liao, J., Pan, X., et al. (2022). Will China's carbon intensity achieve its policy goals by 2030? Dynamic scenario analysis based on STIRPAT-PLS framework. *Science of the Total Environment*, 832, 155060. https://doi.org/10.1016/j.scitotenv.2022.155060

Xie, Z. H., Wu, R., Wang, S. J. (2021). How technological progress affects the carbon emission efficiency? Evidence from national panel quantile regression. *Journal of Cleaner Production*, 307, 127133. https://doi.org/10.1016/j.jclepro.2021.127133

Yang, Y. W., Yan, F. Y., Yang, Y. H., et al. (2023). Evaluating provincial carbon emission characteristics under China's carbon peaking and carbon neutrality goals. *Ecological Indicators*, 156. https://doi.org/10.1016/j.ecolind.2023.111146

York, R., Rosa, E. A., Dietz, T. (2003). STIRPAT, IPAT and ImPACT: analytic tools for unpacking the driving forces of environmental impacts. *Ecological Economics*, 46(3), 351–365. https://doi.org/10.1016/S0921-8009(03)00188-5

Yu, Y., Jian, X., Wang, H., et al. (2024). Unraveling the nexus: China's economic policy uncertainty and carbon emission efficiency through advanced multivariate quantile-on-quantile regression analysis. *Energy Policy*, 188, 114057. https://doi.org/10.1016/j.enpol.2024.114057

Zhan, J., Wang, C., Wang, H., et al. (2024). Pathways to achieve carbon emission peak and carbon neutrality by 2060: A case study in the Beijing-Tianjin-Hebei region, China. *Renewable and Sustainable Energy Reviews*, 189(B), 113955. https://doi.org/10.1016/j.rser.2023.113955

Zhang, K. M., Wen, Z. G. (2008). Review and challenges of policies of environmental protection and sustainable development in China. *Journal of environmental management*, 88(4), 1249–1261. https://doi.org/10.1016/j.jenvman.2007.06.019

Zhang, X., Geng, Y., Shao, S., et al. (2020). How to achieve China's CO_2 emission reduction targets by provincial efforts? – An analysis based on generalized Divisia index and dynamic scenario simulation. *Renewable and Sustainable Energy Reviews*, 127, 109892. https://doi.org/10.1016/j.rser.2020.109892

Zhao, X., Ma, X. W., Chen, B. Y., et al. (2022). Challenges toward carbon neutrality in China: Strategies and countermeasures. *Resources Conservation and Recycling*, 176, 105959. https://doi.org/10.1016/j.resconrec.2021.105959

Zhou, J., Jin, B., Du, S., et al. (2018). Scenario analysis of carbon emissions of Beijing-Tianjin-Hebei. *Energies, 11*(6), 1489. https://doi.org/10.3390/en11061489

Zhou, W., Zeng, B., Wang, J., et al. (2021). Forecasting Chinese carbon emissions using a novel grey rolling prediction model. *Chaos, Solitons & Fractals*, 147, 110968. https://doi.org/10.1016/j.chaos.2021.110968

Zhou, Y., Chen, M., Tang, Z., et al. (2021). Urbanization, land use change, and carbon emissions: Quantitative assessments for city-level carbon emissions in Beijing-Tianjin-Hebei region. *Sustainable Cities and Society*, 66, 102701. https://doi.org/10.1016/j.scs.2020.102701

Zhu, B., Zhang, T. (2021). The impact of cross-region industrial structure optimization on economy, carbon emissions and energy consumption: A case of the Yangtze River Delta. *Science of The Total Environment*, 778, 146089. https://doi.org/10.1016/j.scitotenv.2021.146089